

A Comparative Study with Practical Validation of Photovoltaic Monocrystalline Module for Single and Double Diode Models

Salam J. Yaqoob (✉ engsalamjabr@gmail.com)

Authority of the Popular Crowd

Ameer L. Saleh

University of Misan

Saad Motahhir

Ecole National des sciences appliquées, Université Sidi Med Ben Abdellah, Fes, Morocco.

Ephraim B. Agyekum

Department of Nuclear and Renewable energy, Ural Federal University, 19 Mira Street, Ekaterinburg, Russia.

Research Article

Keywords: Double-diode model, experimental NST-120W, Practical validation, Matlab/Simulink

Posted Date: June 25th, 2021

DOI: <https://doi.org/10.21203/rs.3.rs-605053/v1>

License:  This work is licensed under a Creative Commons Attribution 4.0 International License.

[Read Full License](#)

A Comparative Study with Practical Validation of Photovoltaic Monocrystalline Module for Single and Double Diode Models

Salam J. Yaqoob^{1*}, Ameer L. Saleh², Saad Motahhir³ and Ephraim B. Agyekum⁴

¹Authority of the Popular Crowd, Prime Minister, Iraq.

²College of Engineering, Misan University, Iraq.

³Ecole National des sciences appliquées, Université Sidi Med Ben Abdellah, Fes, Morocco.

⁴Department of Nuclear and Renewable energy, Ural Federal University, 19 Mira Street, Ekaterinburg, Russia.

(Corresponding author Email: engsalamjabr@gmail.com)

Abstract-The photovoltaic (PV) module is equipment that converted sunlight energy to electrical energy. To show the behavior of this device, a mathematical model should be presented. The well-known single-diode and double-diode models were utilized to demonstrate the electrical behavior of the PV module. Moreover, the single and double-diode models have been explained and simulated to study the difference between them under different weather conditions. Furthermore, the mathematical analysis of these models are carried out based on their equivalent circuits. Since, the "Matlab/Simulink" is considered as one of the major software for modeling, analyzing, and solving the dynamic system real problems; it has been used to model and simulate the PV models. In this work the "Mux." and "Fcn." functions in the "Matlab/ Simulink Library" are used which is considered a simple and precise procedure to show the I-V and P-V characteristics. As a result, more accurate results of the I-V and P-V curves have been obtained by the double-diode model compared to the single-diode model. Experimentally, the monocrystalline NST-120W PV module is used to validate the proposed work. The laboratory devices of lux meter, thermometer, ammeter, and voltmeter are used to see the practical results and show the performance of the PV module for different weather conditions. Finally, the experimental voltage, current and power are obtained for the various values of irradiance and temperature through a variable resistive load to obtain the I-V and P-V graphs.

Keywords- Double-diode model, experimental NST-120W, Practical validation, Matlab/Simulink.

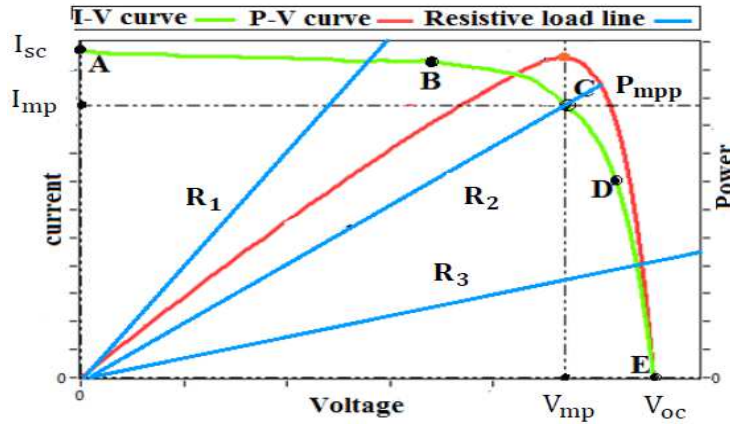
1. Introduction

Today, Renewable energy is the best source of electricity due to having free, clean, and available advantages. Renewable energy gained by PV modules is the most common source [1]. A PV cell is a device that converted sunlight energy to electrical energy, which has a behavior similar to the P-N junction. Actually, the output voltage of these cells should be raised by connecting them in series to form a PV module. It's also connected in parallel to get a large output current. This connection is integrated to form a large PV system with a higher power which is called an array [2]. The PV module's output power primarily depends on irradiation and cell temperature. As a result, whenever the temperature rises, the voltage drops and the current rises slightly. Thus, the PV system efficiency is decreased. Today, different types of PV cell technologies are made on the market, depending on the commercial maturity and manufacturing materials. These types can be summarized into three major technologies, polycrystalline, monocrystalline, and thin-film technologies [3,4]. Polycrystalline technology is not quite efficient due to the arrangement of crystal, which is random, and the cell's color is a little bluer, reflecting more of the sunlight. Monocrystalline technology is extremely efficient. This technology absorbs very high sunlight radiation, as it has a uniform black color. The efficiency of this technology is more than that of polycrystalline. The cost of manufacturing polycrystalline makes this technology cost lower than pure silicon wafers. Thin-film technology is more efficient than other technologies. This technology is made of a thin layer of amorphous film which elicits more energy from the available sunlight. These technologies of the PV cell are combined with the same point in the physics behavior of a diode P-N junction [5-8].

The main drawback of the PV module is the lower efficiency, as a result, a maximum power point tracking (MPPT) was proposed [9-12] to elicit the maximum power and enhance the efficiency of the PV module. Furthermore, the modeling representation of the PV panel is very important to show the PV characteristics under different weather conditions. As a result, many researchers have developed the PV models both single diode and double-diode models and there is a large body of literature on this topic [13,14]. The simple PV model was explored by using a single diode model with four parameters [15,16]. So, the electrical PV module circuit was built using a photo-current source, a diode, a series resistor, and an ideality diode constant. The accuracy of this model is lower compared with that proposed in [17] that added a shunt resistor to achieve a new model with five parameters. Moreover, there is a vast literature on the PV models to solve this issue, in [18-21], a double-diode PV model was presented to increase the accuracy. A photocurrent source, two diodes, a series resistor, a shunt resistor and an ideality diode constant make up this model. Both divisions of the methodology are closely affiliated and have common principles with the different inaccuracies. Similar work has been pursued by authors [22, 23] to develop the double-diode model with an increase in the number of the diodes in parallel, this study may increase the power losses due to the leakage current in the third diode. However, the typical I-V and P-V curves of the PV module are reported in Fig.1.

58 When the terminals of the PV module are short-circuited, the current of a PV module, mathematically equals to
 59 short circuit current ($I_{pv}=I_{sc}$ at $V_{pv} = 0$) which represents the peak produced current value of the PV module.
 60 Furthermore, this current becomes zero while the voltage equals to open-circuit voltage ($I_{pv}=0$ at $V_{pv} = V_{oc}$) when
 61 the terminals of the PV are open-circuited [24]. This voltage represents the peak value of the PV module at no
 62 load. Besides, when a variable resistance load is connected across the PV terminals, the intersection of this load
 63 line with I-V curve represents various operating points on PV curve. So, the slop ($I/V=1/R$) of the characteristics
 64 declare the operating point of the PV module which is represented by (AB) portion, this can be seen if the load
 65 resistance is small (R_1). Also, the operating point extends to point (C), when the load resistance becomes in (R_2),
 66 in this point the maximum power point occurs ($P_{mpp} = I_{mp} \times V_{mp}$). After that, when the load resistance is large
 67 (R_3), the operating point moves to the voltage region (DE) on the I-V curve. Moreover, the resistance of the load
 68 plays an important role to elicit maximum power point from the PV panel. As a result, in the model of PV panel,
 69 the resistance of the load should be adjusted [25-28].

70 In this work, a double-diode model operation is investigated and mathematically compared to a single diode
 71 model. The mathematical equations of these models are built using "Matlab/Simulink". Also, the finding of both
 72 models is achieved and validated in practice in an experiment to show the differences in their characteristics for
 73 the same weather conditions.
 74



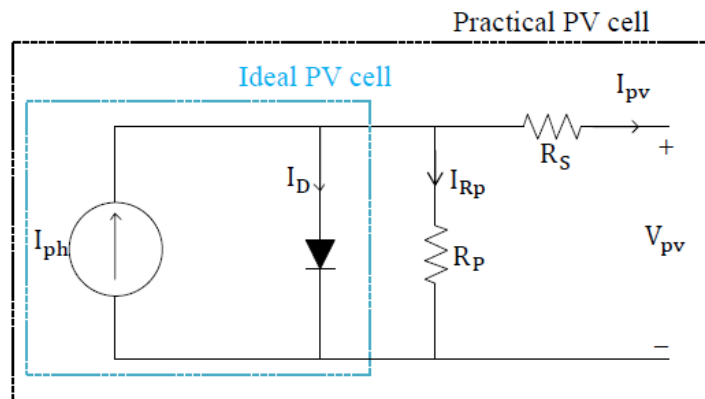
75
76
77
78
79 Fig.1. PV module characteristics.

80 **2. Photovoltaic Cell Models**

81 **2.1 Single-diode Model**

82 The PV cell model as seen in Fig.2, is called a single-diode model because it is built on the assumption that
 83 recombination failure in the depletion area is negligible. The loss of the P-N junction's depletion area is important
 84 which is not visible in the single-diode configuration. Furthermore, the basic equation of semiconductor diode
 theory represents the characteristics of the ideal PV cell as following [9,13]:

85
$$I_{pv} = I_{ph} - I_0 \left[\exp \left(\frac{q V_{pv}}{\alpha K T} \right) - 1 \right]$$
 (1)
 86
 87



88
89
90 Fig.2. single-diode model of the PV cell.

Eq.(1) does not symbolize the real behavior of the PV cell. For this reason, a small milliohm of a series resistor with a high value of a parallel resistor is inserted into the equivalent circuit of the PV cell circuit. The PV cell current can be expressed as [17,18]:

$$I_{pv} = I_{ph} - I_0 \left[\exp \left(\frac{q V_{pv}}{\alpha V_T} \right) - 1 \right] - \frac{V_{pv} + R_s I_{pv}}{R_p} \quad (2)$$

Furthermore, the source of photo-current is linearly proportional to irradiance and it is influenced by temperature as seen in Eq.(3) [20].

$$I_{ph} = (I_{phn} + K_i \Delta T) \frac{G}{G_n} \quad (3)$$

where $\Delta T = T - T_n$ ($T_n = 25^\circ\text{C}$), G is the incident of irradiation on the module and G_n ($1000\text{W}/\text{m}^2$) at STC. Also, the diode saturation current can be written as [16]:

$$I_0 = I_{0n} \left(\frac{T_n}{T} \right)^3 \exp \left[\frac{q E_g}{\alpha K} \left(\frac{1}{T_n} - \frac{1}{T} \right) \right] \quad (4)$$

In general, a modified equation that describes the current in the saturation case as shown below [6].

$$I_0 = \frac{(I_{scn} + K_i \Delta T)}{\exp \left[\frac{(V_{ocn} + K_v \Delta T)}{\alpha V_T} \right] - 1} \quad (5)$$

The aim of this modification makes the open-circuit voltage of the model match that of the experimental. Besides, the saturation current is influenced by the variation of the temperate this modification facilitates the model and eliminates the model's error for open-circuit voltages for regions of the I-V characteristic. The terms of the previous equations are presented as:

- ✓ I_{pv} is the PV output current.
- ✓ V_{pv} is the output voltage of the PV module.
- ✓ I_D is the current of diode.
- ✓ I_{ph} is the photocurrent source.
- ✓ I_0 is the saturation diode current
- ✓ I_{0n} represents the saturation current at STC condition
- ✓ I_{phn} is the photo-current at STC condition
- ✓ T is the ambient temperature
- ✓ $V_T (= N_S K T/q)$ is the voltage of thermal.
- ✓ N_S is the number of cells per module.
- ✓ R_p and R_s are the parallel and series resistances, respectively.
- ✓ K_i is the thermal coefficient at I_{sc} .
- ✓ α is the diode ideality factor
- ✓ K_v is the thermal coefficient at V_{oc} .
- ✓ E_g is the energy of the band gap
- ✓ q is the electron charge ($1.602 \times 10^{-19}\text{C}$)
- ✓ K is the Boltzmann constant $1.3806 \times 10^{-23} \text{J}/^\circ\text{K}$

2.2 Double-diode Model

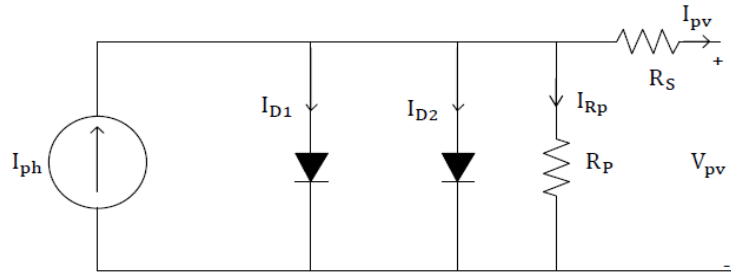
The lack of recombination that is neglected in the single-diode model causes inaccuracy of the PV model parameters. Therefore, the double-diode model as seen in Fig.3 is chosen to represent the physics form of the PV cell. As a result, a more precise model was achieved by accounting for recombination loss. Besides, the diffusion current is focused in the p-n junction material by a single of the double diodes, but the other is added to account for recombination loss [20,21]. Hence, the PV module output current can be defined as:

$$I_{pv} = I_{ph} - I_{D1} - I_{D2} - \left[\frac{V_{pv} + I_{pv} R_s}{R_p} \right] \quad (6)$$

$$I_{D1} = I_{01} \left[\exp \left(\frac{V_{pv} + I_{pv} R_s}{\alpha_1 V_{T1}} \right) - 1 \right] \quad (7)$$

137
138
139

$$I_{D2} = I_{02} \left[\exp \left(\frac{V_{pv} + I_{pv} R_s}{\alpha_2 V_{T2}} \right) - 1 \right] \quad (8)$$



140
141

Fig. 3. Double diode PV model circuit

142 As mentioned before, a more accurate model can be realized using a two-diode model. As a result, seven
143 parameters, namely, I_{ph} , I_{01} , I_{02} , α_1 , α_2 , R_s and R_p must be calculated. Additionally, some studies have
144 used iteration methods to calculate the values of saturation currents for double diode models (I_{01} and I_{02}) [7,8].
145 Generally, I_{01} is about 3–7 orders larger than that of I_{02} . To simplify the calculation, α_1 and α_2 are taken to be
146 1 and 2 respectively. As a result, the saturation currents can be expressed as [14,19]:
147

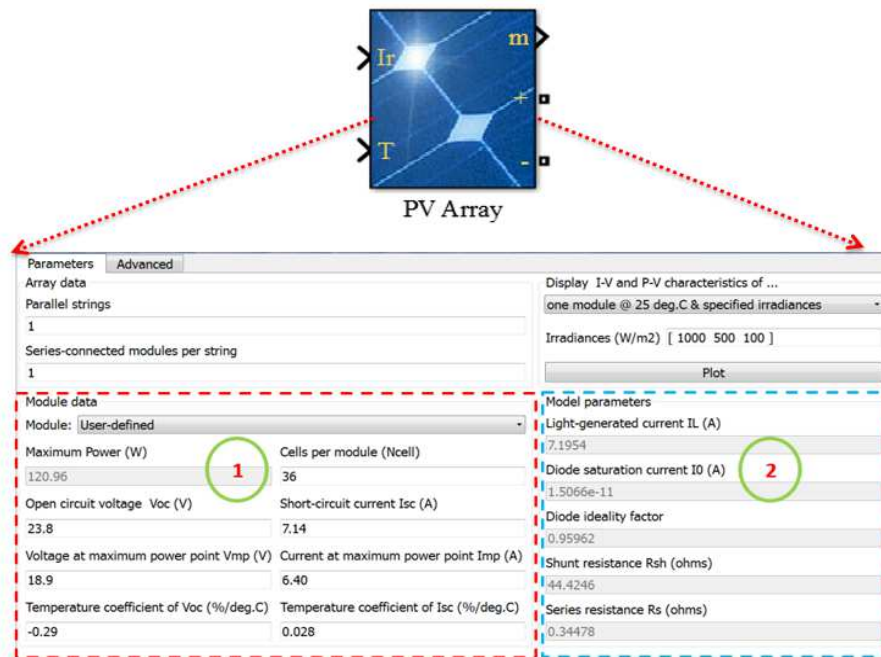
$$I_{01} = \frac{(I_{scn} + K_i \Delta T)}{\exp \left[\frac{(V_{ocn} + K_v \Delta T)}{\alpha_1 V_{T1}} \right] - 1} \quad (9)$$

149

$$I_{02} = \frac{(I_{scn} + K_i \Delta T)}{\exp \left[\frac{(V_{ocn} + K_v \Delta T)}{\alpha_2 V_{T2}} \right] - 1} \quad (10)$$

151 2.3 Extract PV Parameters

152 The PV panel datasheet does not contain some important parameters that are used in the modeling process
153 such as R_s , R_p , I_o , and α . Therefore, in modeling PV panels, these parameters are very important which are used
154 to represent the real circuit of the PV Panel. However, several methods are presented and reviewed to determine
155 these parameters. This paper utilized a simple and sufficient method of PV array Matlab/ tool to compute these
156 parameters. We use this tool that provides in Matlab 2016 version by setting the datasheet parameters by simply
157 clicking on the tool window, the extract parameters are seen as shown in Fig.4. As observed, block (1) refers to
158 the datasheet parameters while block (2) presents the extract PV parameters. Table 1 demonstrates the datasheet
159 parameters of the NST-120 PV panel that is utilized in this paper. The extract parameters are seen in table 2.



160
161
162

Fig.4. extract parameters of the NST-120 panel.

Table 1. Parameters of NST-120 PV panel at STC from datasheet.

Parameter	Value	Unit
P_{mp}	120	W
V_{mp}	18.9	V
I_{mp}	6.40	A
V_{oc}	23.8	V
I_{sc}	7.14	A
K_i	0.028	%/°C
K_V	-0.29	%/°C
N_S	36	-

163
164

Table 2. Extract parameters of the NST-120 PV panel using PV array tool.

Quantity	Value	Unit
R_S	0.344	Ω
R_P	44.42	Ω
I_o	1.5066×10^{-11}	A
α	0.9596	-

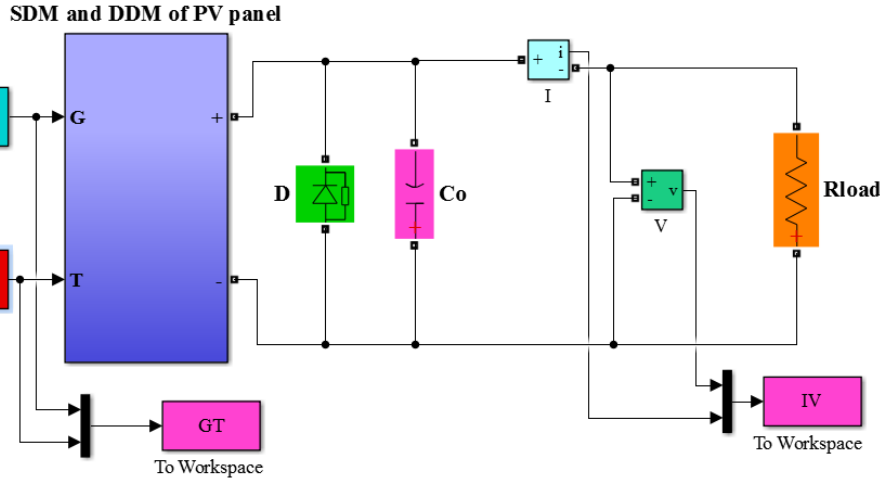
165
166
167
168
169
170

171 **3. Modeling of PV panel**

172 The datasheet and extract parameters of the NST panel are used to simulate the single and double diode models
 173 to represent the P-V and I-V panel characteristics as seen in Fig.5. Also, a simple simulation method of Matlab is
 174 used to see the PV graphs. This method is based on two utilized tools to represent the equations given in section
 175 (2.1) of the single-diode model and the equations given in section (2.2). These models are shown in Figs. (6 and
 176 7) respectively. The two main tools utilized in this work are:

- Multiplexer block (Mux): that is utilized from "library Simulink/Signal Routing".
- Functions block (Fcn): that is utilized from "library Simulink/ User-Defined Functions".

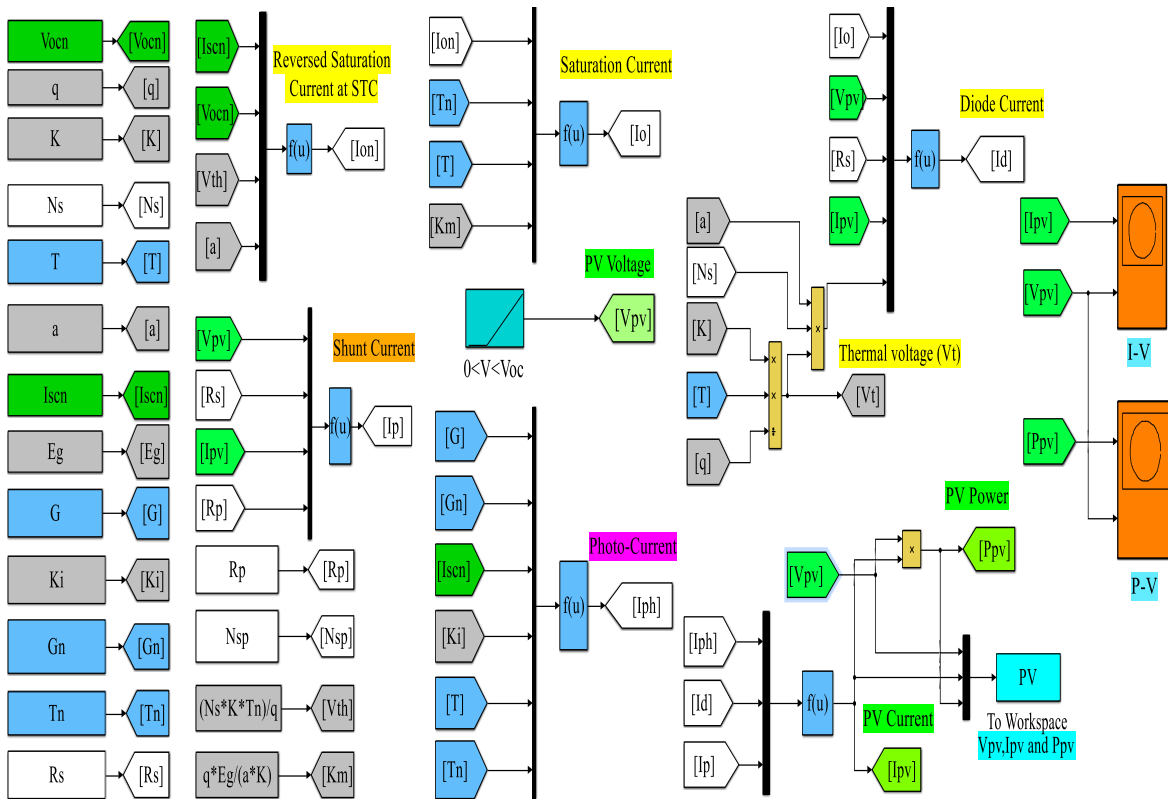
181



182

183

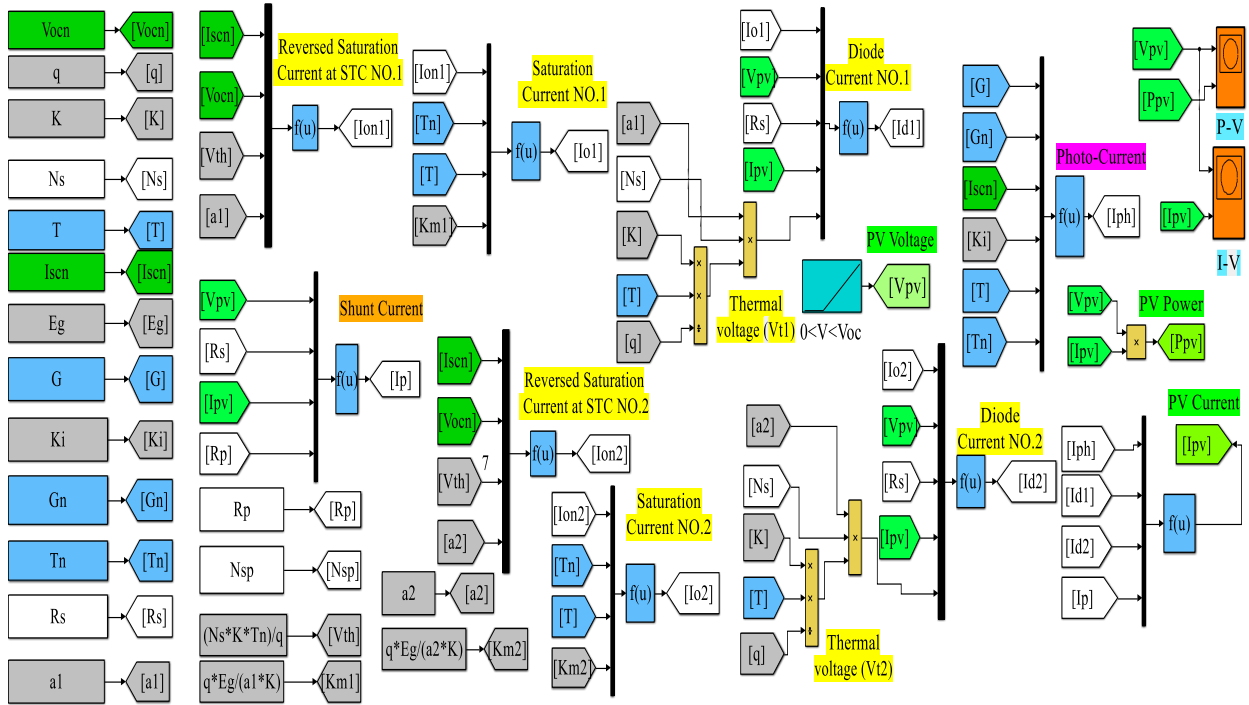
Fig.5 Simulink/Matlab block diagram of the NST-120 PV panel.



184

185

Fig.6. single-diode model block diagram in Matlab.



186

187

Fig.7. double-diode model block diagram in Matlab.

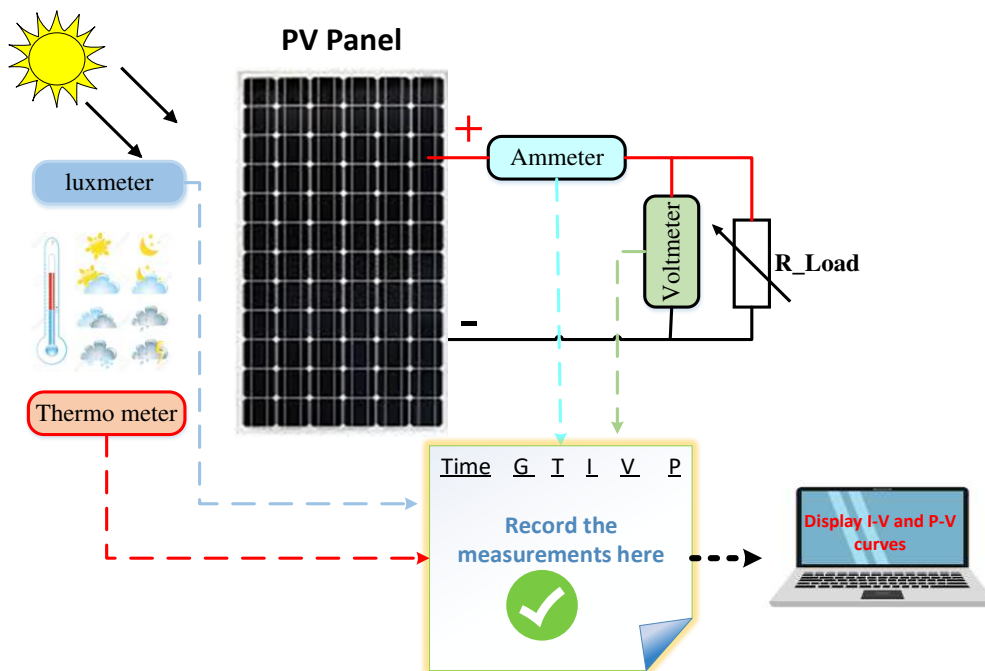
188

189

190 **4. Hardware Implementation**

191 To validate the practical performance of the NST panel for different values of irradiance and temperature, this
 192 panel integrated with the practical measurements devices is seen in Fig.8, this system consists of device lux-meter
 193 device to measure solar irradiance, a thermo-meter device to sense temperature, ammeter, and voltmeter devices.

194



195

196
197
198
199
200
201
202

Fig.8. Proposed PV system components.

4.1 Solar Irradiance Measurement

To show the influence of solar irradiance values on the PV panel performance, a lux-meter device is used to measure irradiance practically. This device is shown the solar irradiance in Lux unit (1Lux-50000 Lux), where every 1 Lux equals 0.79W/m². The manufacturing specifications of this device are shown in Fig.9.



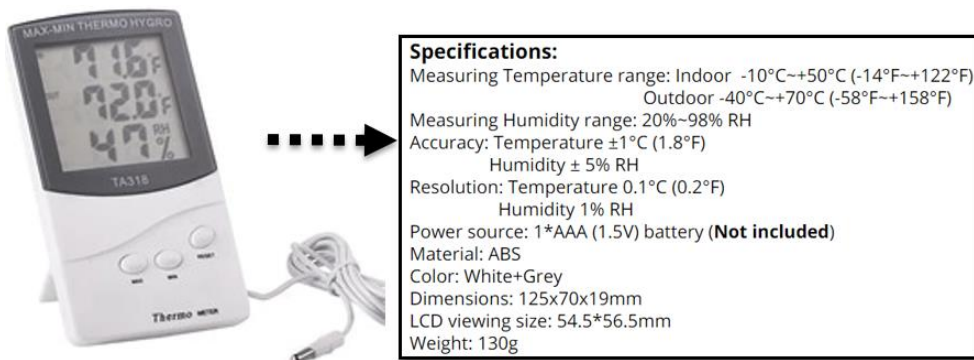
203
204

Fig.9. lux-meter device of solar irradiance.

4.2 Ambient Temperature Measurement

To show the varying ambient temperature in experiment implementation a thermo-meter device is used to measure temperature. The manufacturing specifications of this device are seen in Fig.10. Also, this device offers an additional feature of humidity measurement. This device represents a low-cost simplicity for the user. Besides, the price of the hardware measurement devices utilized in this work is depicted in table 3.

210



211
212

Fig.10 thermo-meter device.

Table 3. Price of hardware devices used in this work (<https://www.aliexpress.com>).

Devices	Description	Price (\$)
Lux meter	Range (1-50000) lux, resolution 1 lux	13.29
Thermometer	Digital indoor/outdoor thermometer hygrometer	3.18
Digital multi meter	DC Voltage range (200mV-1000V), current range (20uA-20A)	10
Total price		26.47

214
215
216

217 **5. Results and Discussion**
 218 **5.1 Simulation Results**

219 In the one-diode model, the obtained simulation results are not sufficient to represent the real PV module
 220 characteristics for different solar insolation and ambient temperature. Besides, the results that have been obtained
 221 by the double diode model are more accurate. Figs. (11 and 12) depict the P-V and I-V graphs for the single-diode
 222 model at STC condition ($T = 25^{\circ}\text{C}$ and $G = 1000\text{W}/\text{m}^2$).

223 Figs. (13 and 14) show the P-V and I-V graphs for double-diode at STC condition. As can be seen that, the
 224 double diodes achieve more accuracy than the single-diode model. Moreover, to see the effects of the irradiance
 225 level and ambient temperature value on the PV characteristics, this model has been tested for different values of
 226 irradiance and temperature as seen in Figs.(15 and 16). Furthermore, when the irradiation increments, the PV panel
 227 voltage is suffered logarithmically while the current increments linearly according to Eq. (3). Also, when the
 228 ambient temperature rises, the voltage reduces due to the sign of K_V which is negative as can be seen below [3]:

229
 230
$$V_{oc} = V_{ocn} + K_V \Delta_T$$
 (11)
 231

232 In addition, the PV current increases slightly to the value of K_i which is a positive sign and very small.

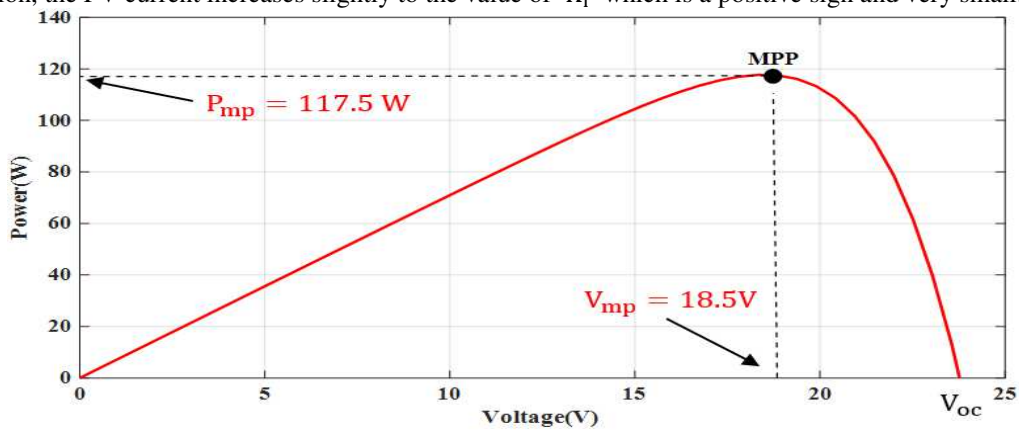
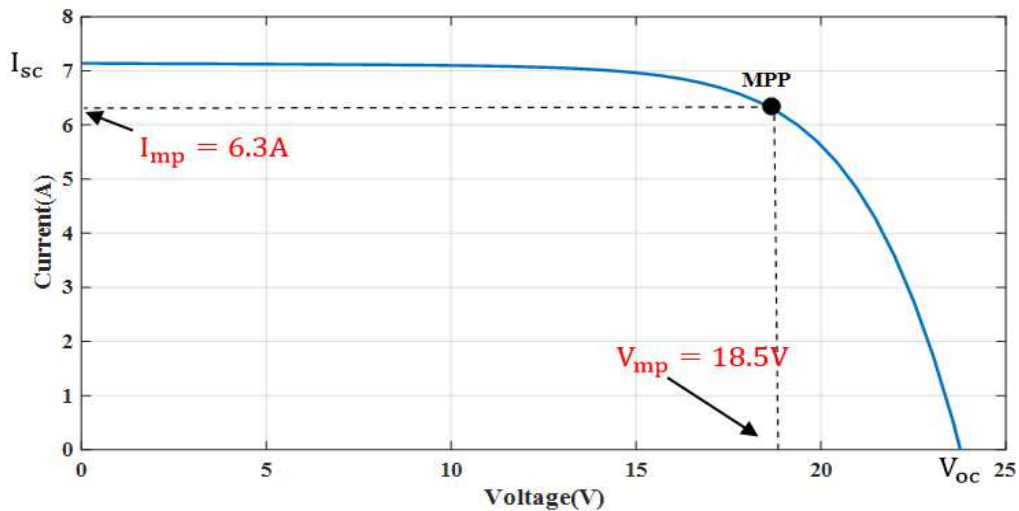
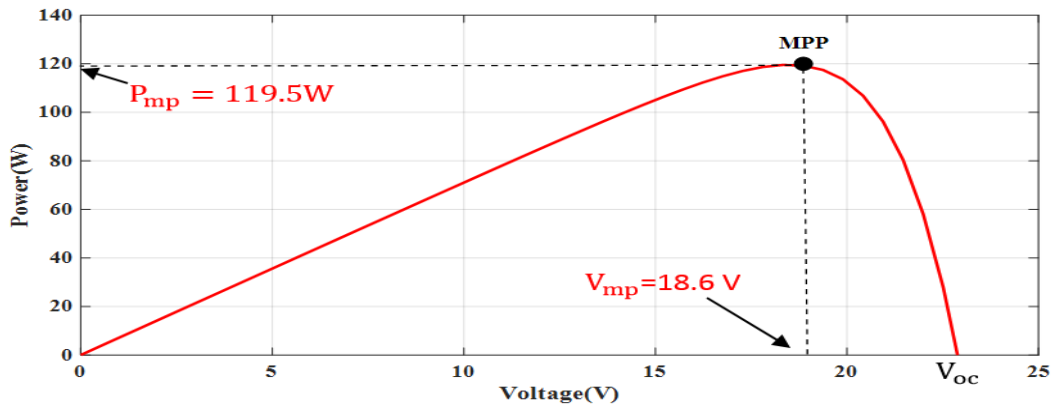


Fig.11. P-V graphs of single-diode model at STC.



. Fig.12. I-V curve of single-diode model at STC.

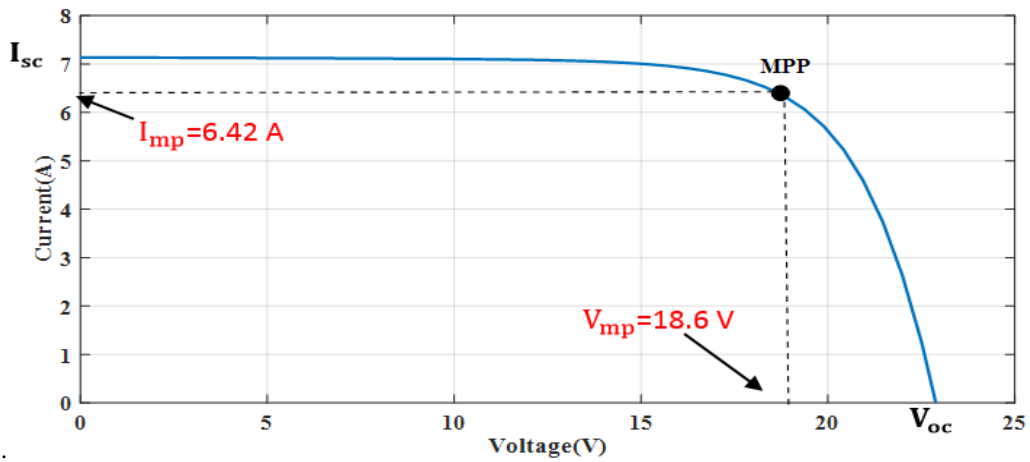


237

238

239

Fig. 13. P-V characteristics of double-diode PV model at STC.



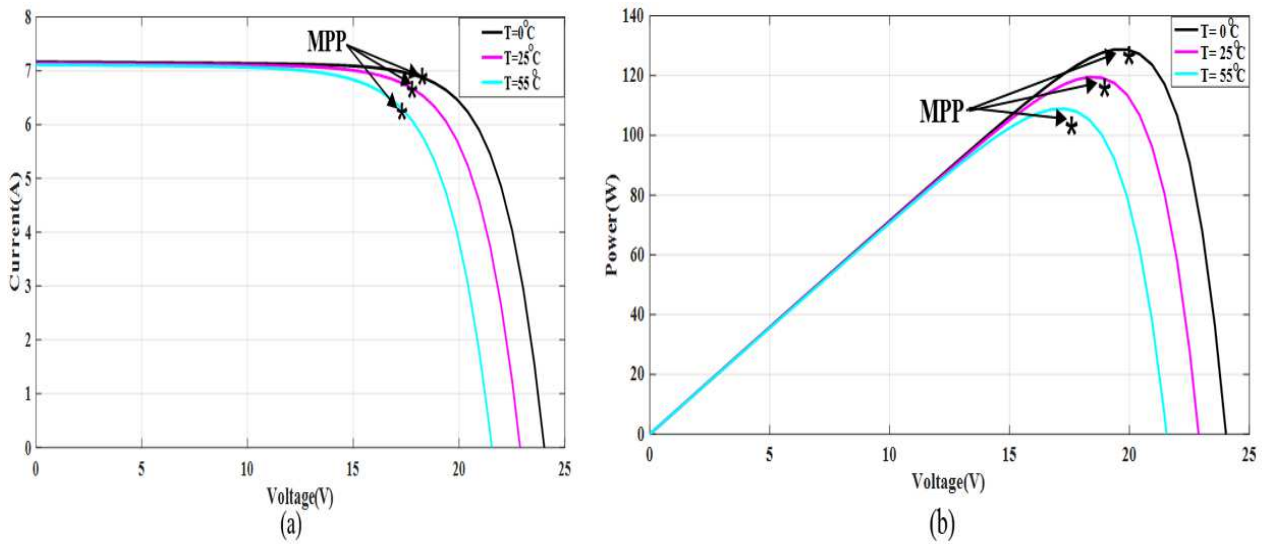
240

241

242

243

Fig. 14. I-V curve of double-diode model at STC.



244

245

246

247

248

249

Fig. 15. I-V and P-V graphs of double-diode model at different values of temperature and fixed irradiation, $G = 1000W/m^2$ (a) I-V graph and (b) P-V graph.

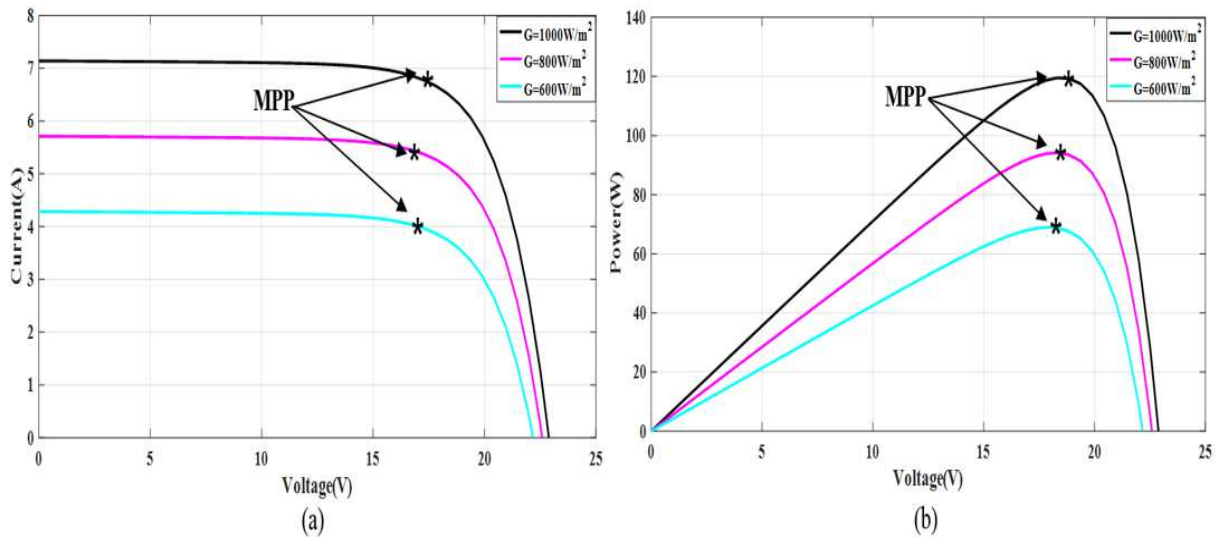


Fig.16 characteristics of double-diode model for different values of irradiation and constant temperature, $T = 25^{\circ}\text{C}$ (a) I-V graph and (b) P-V graph.

5.2 Practical Results

The experimental implementation has been done to show the measurements data (voltage, current, temperature and irradiation) in sun-day for NST-120 PV panel. The experimental voltage, current and power for the PV module are measured with different irradiance and temperature conditions through a variable load to see the I-V and P-V graphs. The experimental components of the PV system are presented in Fig. 17. The photography of measurements in this experiment can be seen in Figs. (18 and 19). The collected data of the real measurements can be observed in Table 4. Also, the PV graphs of its characteristics are seen in Figs (20-22). As observed practically, as irradiation increases, the PV module voltage increases logarithmically while the current increases linearly. Moreover, as temperature increases, the PV module voltage decreases while the current increases slightly as can be seen in Figs. (23 and 24), which depict the NST panel's P-V and I-V curves, respectively.

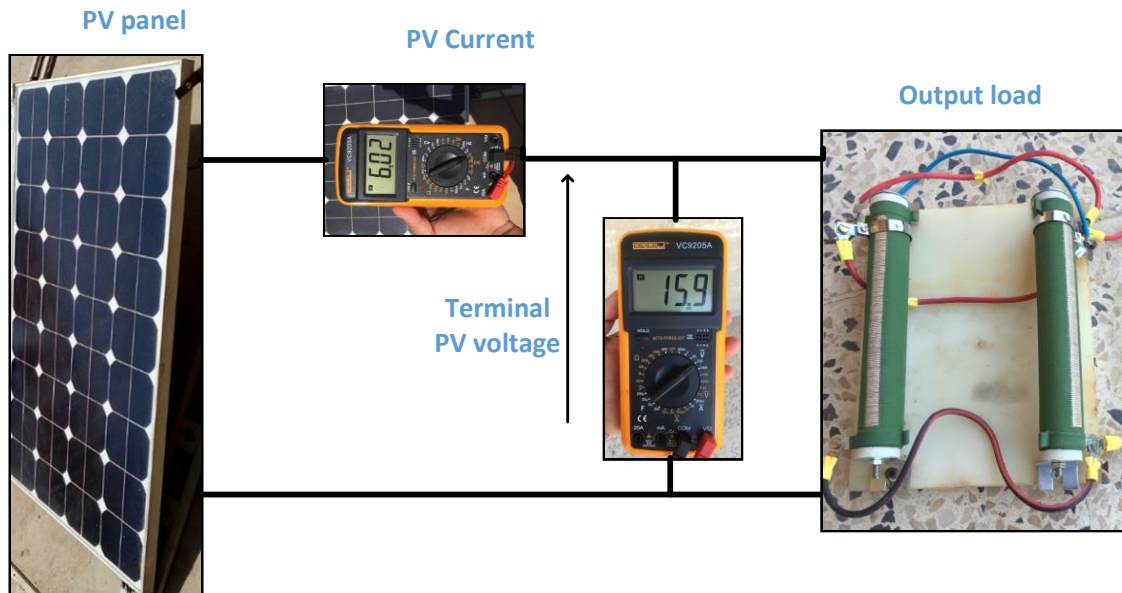


Fig.17. experimental components of proposed system.

271
272

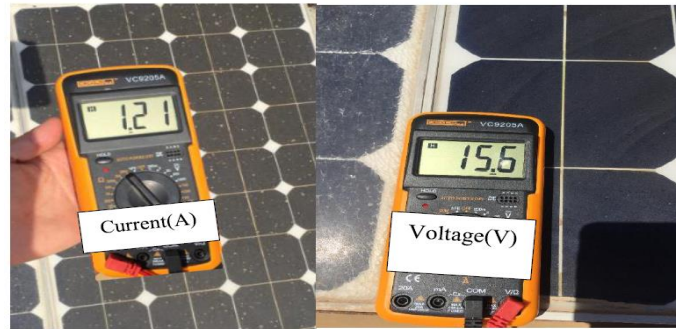


Fig.18. measurements of the current and voltage for the proposed PV system

273
274

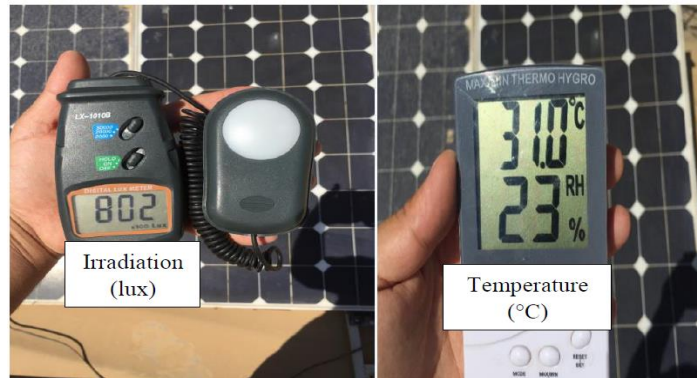


Fig.19. measurements of irradiance and temperature for the proposed PV system.

275
276
277

Table 4. The experimental data for variant weather condition every 1 hour for one sunshine day in (Iraq, Baghdad city).

Time (Hour)	Irradiance (W/m ²)	Temperature (°C)	V (V)	I (A)	P (W)
6:00 am	36	20	14.4	0.3	4.32
7:00 am	153	25	14.6	1.2	17.52
8:00 am	293	28	14.7	2.4	35.28
9:00 am	403	32	14.4	3.16	45.5
10:00 am	530	34	14.28	4	57.12
11:00 am	587	38	14.1	4.39	61.9
12:00 pm	600	40	14.3	4.4	62.92
13:00 pm	578	42	13.96	3.85	53.75
14:00 pm	490	44	14.1	3.17	44.7
15:00 pm	396	43	14.28	2.19	31.27
16:00 pm	260	43	14.18	1	14.18
17:00 pm	125	42	13.68	0.38	5.19
18:00 pm	21	40	12	0.08	0.96

278

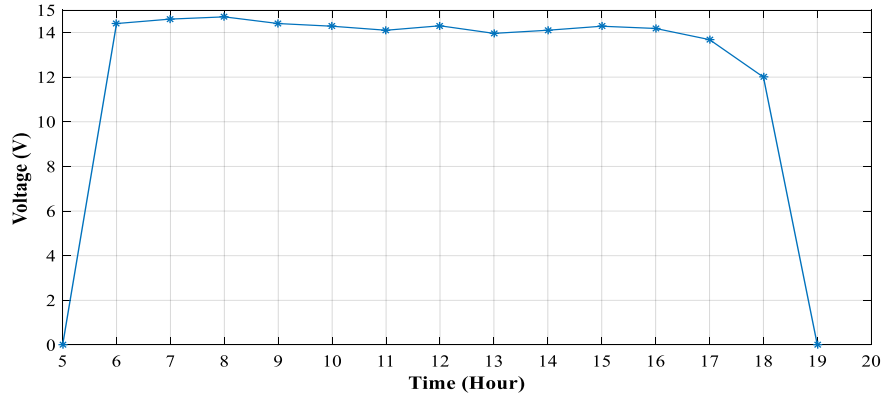


Fig.20. The experimental values of the PV panel voltage.

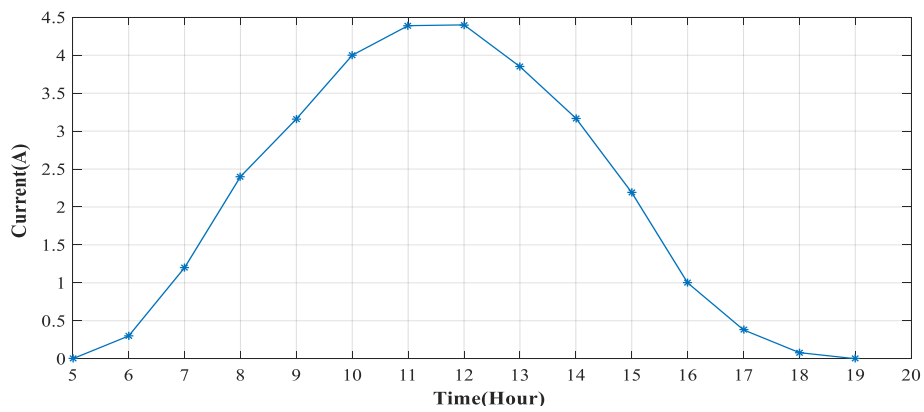


Fig.21. The experimental results of the PV module current.

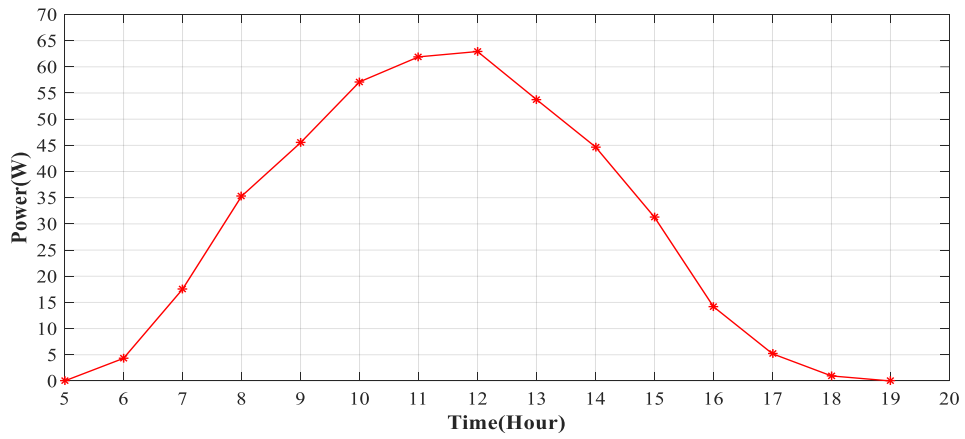


Fig.22. The experimental values of the PV module power.

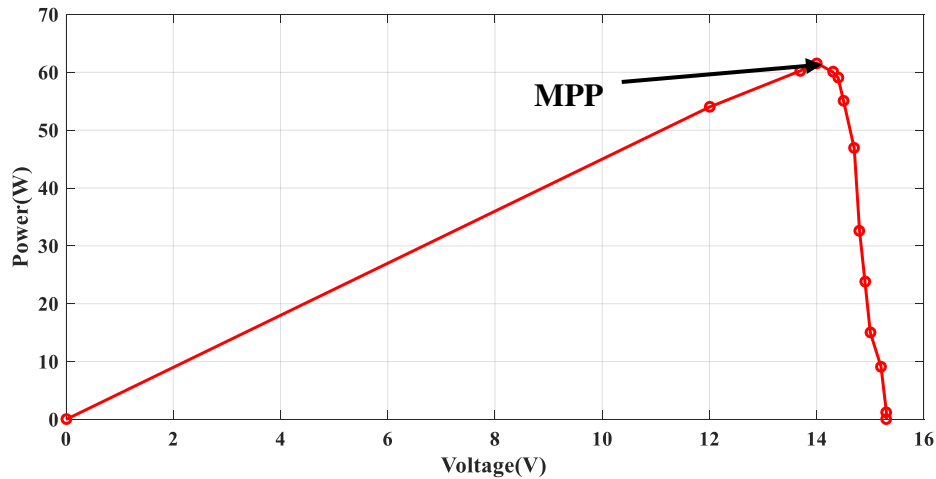


Fig.23. The experimental P-V graphs of the NST PV module.

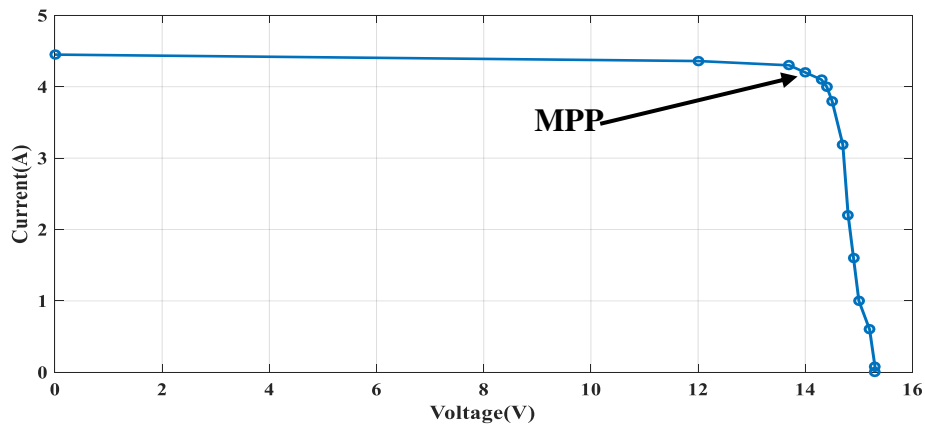


Fig.24. The experimental I-V characteristics of the NST PV module.

6. Conclusion

In this paper, single and double-diode models for modeling the PV module are studied and simulated to depict the difference between them. As a result, the I-V and P-V characteristics of these models are drawn in simulation for various weather conditions. Also, the "Matlab software" has been utilized to simulate both models with two main functions of "Multiplexer and Functions blocks" that are presented in the library of Simulink. The proposed models are validated experimentally using the monocrystalline NST-120W PV module. The experimental results have been obtained during one sunshine day and the I-V and P-V characteristics have been achieved correctly. Hence, from the simulation and experimental results, the double-diode model was more precise than the single-diode model the accuracy of the voltage, current, and power.

Acknowledgments

This research was part of solar PV system project that has received funding from the middle technical university for research and innovation programmer 2020, Iraq.

Data Availability

The data that support the findings of this study are available from the corresponding author upon reasonable request.

References

- [1] V. Quaschnig, "Understanding Renewable Energy Systems," Carl Hanser Verlag GmbH & Co KG, ISBN 1-84407-128-6, London, 2005.
- [2] A. Khaligh and O. Oner, "Energy Harvesting Solar, Wind, and Ocean Energy Conversion Systems," Talyer and Franceis Group, ISBN: 978-1-4398-1508-3, U.S.A, 2010.
- [3] Bagher, Askari Mohammad, Mirzaei Mahmoud Abadi Vahid, and Mirhabibi Mohsen. "Types of solar cells and application " American Journal of optics and Photonics 3.5 (2015): 94-113.
- [4] Imamzai, Mohammadnoor, "A review on comparison between traditional silicon solar cells and thin-film CdTe solar cells." Proceedings of National Graduate Conference (Nat-Grad. 2012.
- [5] Vachtsevanos, G., Kalaitzakis, K., 1987. A hybrid photovoltaic simulator for utility interactive studies. IEEE Trans. Energy Convers. 2, 227–231.
- [6] Walker, G., 2001. Evaluating MPPT converter topologies using a MATLAB PV model. J. Electr. Electron. Eng. 21, 49–56
- [7] Barth, N., Jovanovic, R., Ahzi, S., & Khaleel, M. A. (2016). PV panel single and double diode models: Optimization of the parameters and temperature dependence. Solar Energy Materials and Solar Cells, 148, 87-98.
- [8] Hovinen, A., 1994. Fitting of the solar cell I-V curve to the two diode model. Physica Scripta T54, 2.
- [9] Saleh, Ameer L., Adel A. Obed, Zainab A. Hassoun, Salam J. Yaqoob, "Modeling and Simulation of A Low Cost Perturb& Observe and Incremental Conductance MPPT Techniques In Proteus Software Based on Flyback Converter." IOP Conference Series: Materials Science and Engineering. Vol. 881. No. 1. IOP Publishing, 2020.
- [10] N. Pellet, F. Giordano, M. Ibrahim Dar, G. Zakeeruddin, S. M., Maier, and M. Grätzel, "Hill Climbing Hysteresis of Perovskite-based Solar Cells: a Maximum Power Point Tracking Investigation," Progress in Photovoltaics: Research and Applications Vol.25, No.11, pp.942-2017.950.
- [11] M. Kermadi, and El M. Berkouk, "Artificial intelligence-based Maximum Power Point Tracking Controllers for Photovoltaic Systems: Comparative study," Elsevier publisher, Renewable and Sustainable Energy Reviews Vol.69, pp.369-386, Nov. 2017.
- [12] Farzaneh, J., Keypour, R., & Khanesar, M. A. (2018). A new maximum power point tracking based on modified firefly algorithm for PV system under partial shading conditions. Technology and Economics of Smart Grids and Sustainable Energy, 3(1), 1-13.
- [13] Laudani, A., Riganti Fulginei, F., Salvini, A., 2014. Identification of the one-diode model for photovoltaic modules from datasheet values. Sol. Energy 108, 432–446. <http://dx.doi.org/10.1016/j.solener.2014.07.024>.
- [14] Kashif-Ishaque, Zainal-Salam, and Hamed-Taheri, "Accurate MATLAB Simulink PV System Simulator Based on a Two-Diode Model," Elsevier publisher. Journal of Power Electronics. vol.11. pp.11-2-9. March.2011.
- [15] Motahhir, S., Chalh, A., Ghzizal, A., Sebti, S., & Derouich, A. (2017). Modeling of photovoltaic panel by using proteus. Journal of Engineering Science and Technology Review, 10, 8-13.
- [16] Lu, D. D., & Nguyen, Q. N. (2012). A photovoltaic panel emulator using a buck-boost DC/DC converter and a low cost micro-controller. Solar Energy, 86(5), 1477-1484.

- [17] V. L. Brano, A. Orioli, G. Ciulla and A. D. Gangi, "An improved Five-parameter Model for Photovoltaic Modules " Elsevier publisher, *Renewable and Sustainable Energy Reviews*. vol.61. pp. 354-371, Mar. 2016.
- [18] A. Rezaee Jordehi, "Parameter Estimation of Solar Photovoltaic (PV) Cells: A review" Elsevier publisher, *Renewable and Sustainable Energy Reviews*, vol.61, pp. 354-371, Mar. 2016.
- [19] L. Sandrolini, M. Artioli, U. Reggiani, "Numerical method for the extraction of photovoltaic module double-diode model parameters through cluster analysis," Elsevier publisher. *Applied Energy*. vol.87. pp.442-451, Sep.2010.
- [20] Salam J. Yaqoob, and Adel A. Obed, "Modeling, Simulation and Implementation of Photovoltaic Panel Model by Proteus Software Based on High Accuracy Two-diode Model," *Journal of Techniques*, Vol.1, No.1. pp.39-51, Des., 2019.
- [21] Chin, Vun Jack, and Z. Salam. "Modifications to Accelerate the Iterative Algorithm for the Two-diode Model of PV Module," *IEEE PES Asia-Pacific Power and Energy Engineering Conference (APPEEC)*, Oct. 2018.
- [22] Khanna, V., Das, B. K., Bisht, D., & Singh, P. K. (2015). A three diode model for industrial solar cells and estimation of solar cell parameters using PSO algorithm. *Renewable Energy*, 78, 105-113.
- [23] Nishioka, K., Sakitani, N., Uraoka, Y., & Fuyuki, T. (2007). Analysis of multicrystalline silicon solar cells by modified 3-diode equivalent circuit model taking leakage current through periphery into consideration. *Solar energy materials and solar cells*, 91(13), 1222-1227.
- [24] Nasser, K. W., Yaqoob, S. J., & Hassoun, Z. A. (2021). Improved dynamic performance of photovoltaic panel using fuzzy logic-MPPT algorithm. *Indonesian Journal of Electrical Engineering and Computer Science*, 21(2), 617-624.
- [25] De Brito, M. A. G., Galotto, L., Sampaio, L. P., e Melo, G. D. A., & Canesin, C. A. (2012). Evaluation of the main MPPT techniques for photovoltaic applications. *IEEE transactions on industrial electronics*, 60(3), 1156-1167.
- [26] Chalh, A., Motahhir, S., El Hammoumi, A., El Ghzizal, A., & Derouich, A. (2018). Study of a low-cost PV emulator for testing MPPT algorithm under fast irradiation and temperature change. *Technology and Economics of Smart Grids and Sustainable Energy*, 3(1), 1-10.
- [27] El Hammoumi A, Motahhir S, Chalh A, El Ghzizal A, Derouich A (2018) Low-cost virtual instrumentation of PV panel characteristics using Excel and Arduino in comparison with traditional instrumentation. *Renew Wind Water Sol* 5(1):3.
- [28] Errouha, M., Derouich, A., Motahhir, S. et al. Optimal Control of Induction Motor for Photovoltaic Water Pumping System. *Technol Econ Smart Grids Sustain Energy* 5, 6 (2020). <https://doi.org/10.1007/s40866-020-0078-9>.

Author Contribution

Author 1: Salam J. Yaqoob

- Conceived and designed the analysis
- Collected the data
- Wrote the paper

Author 2: Ameer L. Saleh

- Performed the analysis

Author 3: Saad Motahhir

- Improve the writing of the paper
- Performed the analysis

Author 4: Ephraim B. Agyekum

- Improve the writing of the paper
- prepared the figures